SPACECRAFT ATTITUDE DETERMINATION BASED ON GPS CARRIER PHASE MEASUREMENTS

Evrim Özten[1]
Middle East Technical University
Ankara, Turkey

Ozan Tekinalp[2]
Middle East Technical University
Ankara, Turkey

ABSTRACT

This paper presents an Extended Kalman Filter (EKF) algorithm in order to estimate spacecraft attitude using Global Positioning System (GPS) carrier phase measurements. The algorithm is implemented using an error state vector including three quaternion and three inertial angular velocity error states. A simulation is developed to evaluate the performance of the algorithm. GPS carrier phase measurements are modeled in the simulation environment. An integrated GPS and 3-axis gyro attitude determination algorithm is also presented in this paper. The algorithms designed for the GPS only and GPS/Gyro integrated cases are tested with different GPS visibility conditions.

INTRODUCTION

The Global Positioning System (GPS) is a space-based radio positioning and time transfer system. Over the past years, GPS receivers have been used in the land, sea, air and even in the space applications for the position, velocity and time determination purposes. With the further improvements in the GPS technology, it has been proven that not only the positioning information, but also the attitude knowledge can be derived from the GPS signals with the accuracy less than 1 degree [Bak, 1999]. Because almost all the satellites are equipped with GPS receivers for the position determination, the replacement of other attitude sensors with the GPS receiver provide advantages in terms of cost and reliability.

In this study, the development of a GPS based attitude determination is aimed. An estimation algorithm is developed in the MATLAB Simulink environment for the attitude determination using the GPS carrier phase measurements from four antennas. Because the measurement model and the satellite attitude dynamics for this study are nonlinear, Extended Kalman Filter (EKF), a nonlinear estimator, is decided to use. The algorithm is implemented using three quaternion and three inertial angular velocity error states. For the attitude determination, four antennas in a square shape with 1 meter inter-antenna distance are assumed to be used.

In this study, a simulation is conducted in order to evaluate the performance of the algorithm. The simulation includes a satellite in J_2 perturbed orbit. The yaw stabilization of the satellite is maintained by using a momentum wheel with spin axis perpendicular to the orbit plane. GPS differential carrier phase measurements are also modeled in the simulation environment. Because most of the measurement errors are quite small in the carrier phase measurement or they are mostly cancelled out after the single differencing process, only the multipath error and receiver noise is modeled in the simulation. Errors due to integer ambiguity are not investigated in this study. This error is assumed to be correctly solved before the attitude determination process.

The fundamental problem of using GPS based attitude determination system is the low output rate which may not be enough to obtain accurate attitude solutions for the satellites with rapidly changing attitudes such as spinning satellites. The other problem is the loss of GPS satellite visibility due to the direction of the aligned antenna array. The problem of low GPS satellite visibility might also be arisen for the high altitude satellites. For such cases, GPS based systems cannot meet the high accuracy

[1] M.Sc. Student in Aerospace Engineering Department, Email: e144969@metu.edu.tr
[2] Prof. in Aerospace Engineering Department, Email: tekinalp@metu.edu.tr

requirement. Therefore, an integrated system with high rate aiding sensors should be considered for such systems. In this paper, the details for an attitude determination algorithm considering an integrated GPS and three-axis gyro case are also presented. For the integrated GPS/Gyro case, the developed EKF is modified by adding gyro bias drift parameter to the state vector. In order to model the gyro measurements, a gyroscope error model is developed. The gyro measurements are generated by adding errors like bias drift, scale factor and misalignment to the true angular rates.

The algorithms developed for GPS only and GPS/Gyro integrated cases are tested with different GPS visibility conditions.

SIMULATION DEVELOPMENT

The flow chart of the simulation developed is given in the Figure 1. In the first step of the simulation, an initialization process is required. The parameters required in this step are given in Table 1.

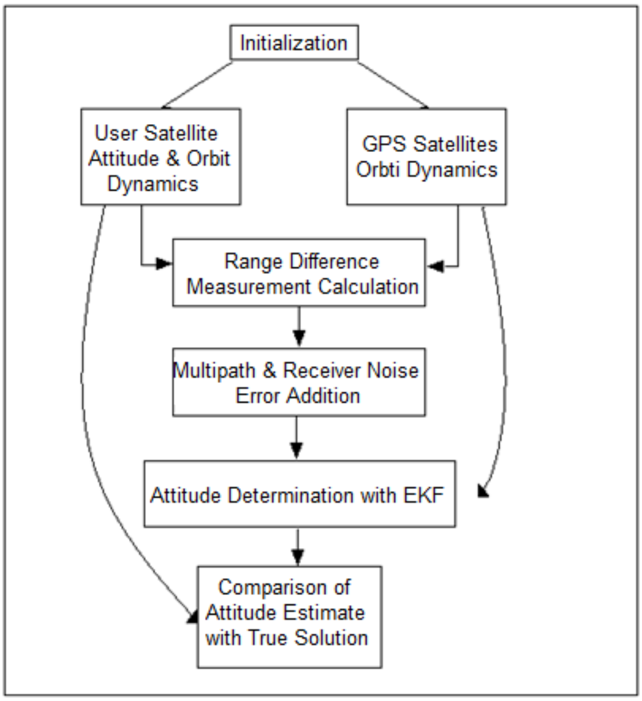

Figure 1: Flow Chart of the Simulation

Table 1: User Satellite Parameters and Initial Conditions

USER SATELLITE PARAMETERS			
ORBITAL ELEMENTS		**SATELLITE CONFIGURATION**	
Semi-major axis	7000 km	Moment of Inertia	I=1000,1500,2000kg m2
Eccentricity	0.00145	Momentum wheel	50 kg m2/s
Inclination	98 degrees	Nbr. Of Antennas	4
Argument of Perigee	237 degrees	Baseline	1m
RAAN	8.8 degrees		
True Anomaly	0		
SIMULATION INITIALIZATION			
INITIAL CONDITIONS		**MEASUREMENT ERRORS**	
Initial Euler Angles	3 degrees for three axes	Receiver Noise on the Range Difference	σ = 1 mm
Initial Euler Angle Error	3 degrees for three axes		
Initial Angular Velocity	0.005 deg/s for three axes	Multipath on the Range Difference	σ = 2 mm with 300 sec. time constant
Initial Angular Velocity	0.005 deg/s for three axes		
Initial Position Error	1 m for three axes		
Initial Velocity Error	0.01 m/s for three axes		

Using the parameters given in Table 1, the true attitude solution of the satellite is obtained using equations of the motion (eq.6 and eq.9). The results for the one period of its flight are given in Figure 2. The estimated solutions are compared with the true solution given.

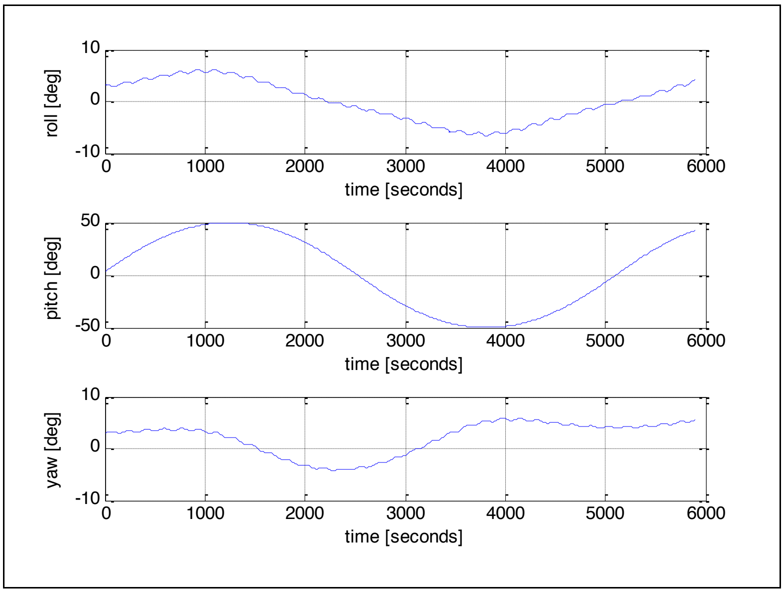

Figure 2: True Euler Angles

Coordinate Systems

For this study, three reference frames are defined as shown in Figure 3. Because the angular velocity and attitude propagation is carried out in the inertial frame, it is the first frame that is needed to be defined. The inertial frame, denoted by **I**, is considered as a non-accelerated, non-rotated reference frame in which Newton's laws is valid. It is centered at the Earth's center of mass. $\mathbf{Z}^I$ is aligned with the Earth's spin axis, $\mathbf{X}^I$ is pointing towards vernal equinox and $\mathbf{Y}^I$ completes the right-handed orthogonal set.

The attitude of a spacecraft is the orientation of its body fixed coordinate system with respect to a reference coordinate system in space. In this study, the attitude is defined between body fixed frame and orbit level frame. Therefore, these are the other frames used in this study. Orbit level coordinate system is centered at the spacecraft's center of mass. $\mathbf{Z}^L$ is directed toward the nadir, $\mathbf{Y}^L$ is along the negative orbit normal and $\mathbf{X}^L$ completes the orthogonal right-handed set.

The body fixed coordinate system, denoted by **B**, is fixed relative to the spacecraft body. Its origin is placed at the spacecraft mass center. The body frame coordinate system axes are directed such that the roll, pitch and yaw angles are zero when the body fixed frame is perfectly aligned with the orbit level frame. The yaw, pitch and roll angles of the spacecraft is defined as the rotation angles while transforming the local level frame to the body fixed frame in the Z-Y-X rotation order respectively. It is assumed that the axes of body frame coincide with the principle axes of the spacecraft.

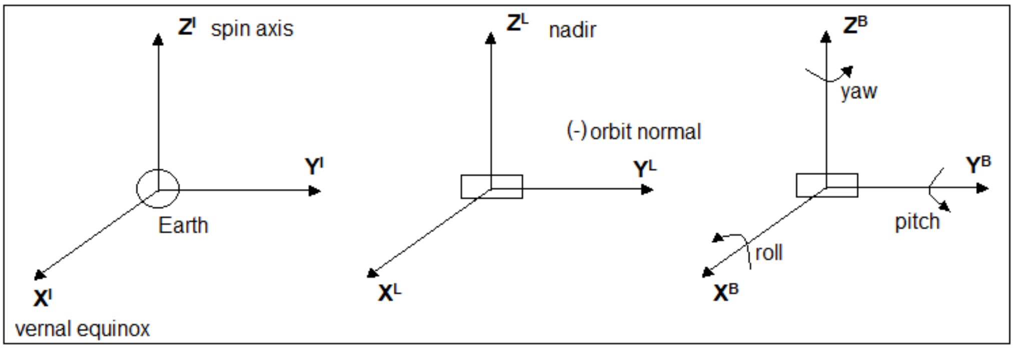

Figure 3: Inertial, Orbit Level and Body Fixed Coordinate Systems

Then, the transformation from the orbit level coordinate system to the body fixed coordinate system can be performed with the rotation matrix, R_L^B [Titterton, 2004]:

$$R_L^B = \begin{bmatrix} {q_0}^2 + {q_1}^2 - {q_2}^2 - {q_3}^2 & 2(q_1q_2 + q_0q_3) & 2(q_1q_3 - q_0q_2) \\ 2(q_1q_2 - q_0q_3) & {q_0}^2 - {q_1}^2 + {q_2}^2 - {q_3}^2 & 2(q_2q_3 + q_0q_1) \\ 2(q_1q_3 + q_0q_2) & 2(q_2q_3 - q_0q_1) & {q_0}^2 - {q_1}^2 - {q_2}^2 + {q_3}^2 \end{bmatrix} \tag{1}$$

Orbit Dynamics

In the simulation, the true motion of the user satellite is described by using two-body orbital mechanics with the effects of the second zonal harmonics, J_2. The second zonal harmonic is a zonal harmonic coefficient in an infinite Jacobi Polynomial series representation of the Earth's gravity field. It represents the dominant effects of Earth oblateness and has the value of 1.082629×10^{-3}. The other harmonics are at least 1000 times smaller than J_2.

The equations of the motion are [Anton, 2013]:

$$\begin{aligned} \ddot{x} &= \frac{-\mu x}{r^3}\left[1 - \frac{3}{2}J_2\left(\frac{R_e}{r}\right)^2\left(5\frac{z^2}{r^2} - 1\right)\right] \\ \ddot{y} &= \frac{-\mu y}{r^3}\left[1 - \frac{3}{2}J_2\left(\frac{R_e}{r}\right)^2\left(5\frac{z^2}{r^2} - 1\right)\right] \\ \ddot{z} &= \frac{-\mu z}{r^3}\left[1 - \frac{3}{2}J_2\left(\frac{R_e}{r}\right)^2\left(5\frac{z^2}{r^2} - 3\right)\right] \end{aligned} \tag{2}$$

where $\mathrm{r} = \sqrt{\mathrm{x}^2 + \mathrm{y}^2 + \mathrm{z}^2}$ and x, y, z are satellite position coordinates with respect to the inertial frame, $\mathrm{R_e}$ is the Earth radius, μ is the Earth's gravitational constant, and J_2 is the Earth's 2nd order zonal harmonics.

On the other hand, the position and velocity of the GPS satellites are calculated by considering only the two-body effects in the simulation due to their high altitude.

Attitude Dynamics

In the simulation, the satellite body is assumed to be a rigid body. The rotational equations of motion for a rigid body can be expressed by Euler's equation:

$$\dot{\boldsymbol{h}} + \boldsymbol{\omega}\times\boldsymbol{h} = \boldsymbol{M} \tag{3}$$

where $\mathbf{h}$ is the angular momentum vector of the spacecraft, $\boldsymbol{\omega}$ is the inertial angular velocity vector and $\mathbf{M}$ is the net applied moment about the mass center.

During this study, it is assumed that the net moment acting on the satellite body is only the gravity gradient torque, $\mathbf{M_{GG}}$.

$$\boldsymbol{M} = \boldsymbol{M_{GG}} = \frac{3\mu}{r^3}\hat{\boldsymbol{r}}\times(I\hat{\boldsymbol{r}}) \tag{4}$$

In order to ensure the yaw stabilization of the satellite, it is assumed that a constant speed momentum wheel with the spin axis perpendicular to the orbit plane is attached to the satellite. Then the total angular momentum, $\mathbf{h}$, can be expressed as:

$$\boldsymbol{h} = I\boldsymbol{\omega} + \boldsymbol{h_w} \tag{5}$$

,where r is the satellite orbit radius, $\hat{\mathbf{r}}$ is the unit vector in the radial direction, I is the moment of inertia, μ is Earth's gravitational constant with the value of $398600.4415\ \mathrm{km^3/s^2}$, $\mathbf{h_w}$ is the angular momentum vector due to the momentum wheel and it is equal to $\mathbf{h_w} = -\mathrm{h_w}\mathbf{j^B}$.

After inserting eq.(4) and eq.(5) into the eq.(3), the inertial angular velocity propagation equations are obtained. ω_1, ω_2 and ω_3 represents the inertial angular velocity along the $\mathbf{i^B}, \mathbf{j^B}$ and $\mathbf{k^B}$ axes respectively. R represents the orbit level to body fixed coordinate system transformation matrix as given in eq.(1). $R_{\alpha,\beta}$ represents the element in the row α and column β.

$$\dot{\omega}_1 = \frac{(I_2 - I_3)}{I_1}\left[\omega_2\omega_3 - \frac{3\mu}{r^3}R_{2,1}R_{3,1}\right] - \omega_3\frac{h_w}{I_1}$$
$$\dot{\omega}_2 = \frac{(I_3 - I_1)}{I_2}\left[\omega_1\omega_3 - \frac{3\mu}{r^3}R_{1,1}R_{3,1}\right] \tag{6}$$
$$\dot{\omega}_3 = \frac{(I_1 - I_2)}{I_3}\left[\omega_1\omega_2 - \frac{3\mu}{r^3}R_{1,1}R_{2,1}\right] + \omega_1\frac{h_w}{I_3}$$

After the inertial velocities are obtained, they are used to propagate the spacecraft attitude in the simulation. The attitude propagation is performed with the following equation:

$$\dot{q} = 0.5\, q \otimes p_{LB}^{B} \tag{7}$$

,where $p_{LB}^{B} = \left[0 \quad \omega_{LB}^{B\,T}\right]^{T}$, ω_{LB}^{B} is the angular velocity with respect to the orbit level frame expressed in the body fixed coordinate system, and the operator '⊗' refers to the quaternion multiplication.

Because the angular velocity of the spacecraft is obtained with respect to the inertial frame (ω_{IB}^{B}) through the Euler's equation, it is more convenient to remove the angular velocity of orbit level frame with respect to the inertial frame (ω_{IL}^{B}):

$$\omega_{LB}^{B} = \omega_{IB}^{B} - \omega_{IL}^{B} \tag{8}$$

,where $\omega_{IL}^{B} = R_{L}^{B}\omega_{IL}^{L}$, $\omega_{IL}^{L} = [0 \quad -\dot{u} \quad 0]^{T}$ and u refers to the argument of latitude.

The quaternion propagation equations are then obtained as:

$$\dot{q}_0 = -0.5[q_1\omega_1 + q_2(\omega_2 + \dot{u}) + q_3\omega_3]$$
$$\dot{q}_1 = \quad 0.5[q_0\omega_1 + q_2\omega_3 - q_3(\omega_2 - \dot{u})]$$
$$\dot{q}_2 = \quad 0.5[q_0(\omega_2 + \dot{u}) - q_1\omega_3 + q_3\omega_1] \tag{9}$$
$$\dot{q}_3 = \quad 0.5[q_0\omega_3 + q_1(\omega_2 - \dot{u}) - q_2\omega_1]$$

GPS Observations

GPS based attitude determination is based on the phase difference measurements, $\Delta\varphi$, between the signals received by a master antenna and one or more slave antennas.

The phase difference measurements ($\Delta\varphi$) can be related to the range difference (Δr) as eq.(10). Therefore, the range difference can be calculated using the measured phase difference, after resolving the integer ambiguity n, and the constant hardware delay, β [Lightsey, 2004].

$$\Delta r = \Delta\varphi + n - \beta + \epsilon \tag{10}$$

,where ϵ is the measurement error.

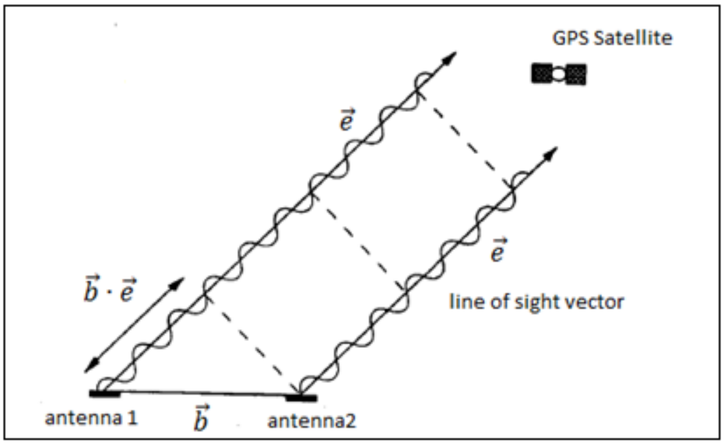

Figure 4: GPS Carrier Phase Geometry

The range difference can be described as the projection of the baseline vector (**b**) onto the line of sight vector from the antenna to the GPS satellite (**e**) as shown in Figure 4 .

$$\Delta r = \boldsymbol{b} \cdot \boldsymbol{e} + \epsilon \tag{11}$$

It is more convenient to obtain the baseline vector in the body fixed coordinate system, and the line-of-sight vector is known in the inertial frame. Then the range difference equation in the matrix form becomes as the following equation:

$$\Delta r = (b^B)^T R_I^B e^I + \epsilon \tag{12}$$

,where $\mathrm{R_I^B}$ is the transformation matrix from inertia to the body fixed coordinate system, and it is obtained by $\mathrm{R_I^B = R_L^B R_I^L}$

Then the final form of the equation becomes:

$$\Delta r = (b^B)^T R_L^B R_I^L e^I + \epsilon \tag{13}$$

Because the satellite attitude is defined as the orientation of the body fixed frame with respect to the orbit level frame, the term R_L^B in the equation above relates the range difference with the attitude of the satellite. In this study, the attitude is estimated from the calculated range difference. These measurements are generated in the simulation using eq.(13) by assuming that integer ambiguity and hardware delay problems are perfectly solved. Because most of the measurement errors are quite small in the carrier phase measurement or they are mostly cancelled out after the single differencing process, only the receiver noise and multipath error is modeled in the simulation. The receiver noise is assumed to have a Gaussian White Noise distribution, while a first order Gauss-Markov process is used in order to represent the multipath error [Khanafseh, 2010].

Gyro Measurements

The gyro measurements are simulated by adding sensor errors, namely bias stability, space factor, misalignment and random noise, to the true angular velocities calculated through attitude dynamics. The sensor error characteristics given in Table 2 are used in the gyro error model. These values belong to a typical MEMS gyro for the space applications [Brady, 2012].

Table 2: Gyro Properties

Parameter	1σ Values
Bias Stability [deg/hr]	1.0
Scale Factor Repeatability [ppm]	30
Misalignment [μrad]	100
Anglular Random Walk [deg/$\sqrt{\mathrm{hr}}$]	0.01

ATTITUDE ESTIMATION

In this study, two Extended Kalman Filter (EKF) algorithms are developed in order to estimate the spacecraft attitude. One of them is based on standalone GPS measurements. The other one includes a system with integrated GPS and three-axis gyroscope.

The Kalman Filter is composed of three steps. The first step is the state and error covariance propagation in time. Then, the Kalman gain calculation is performed using the propagated state vector and covariance matrix. Finally, the measurements are used in order to correct the propagated states and their covariance.

The general equations for a Kalman filter are presented below [Groves, 2008]:

Time Update Equations	$x_k^- = \Phi_{k-1} x_{k-1}^+$
	$P_k^- = \Phi_{k-1} P_{k-1} \Phi_{k-1}^T + Q$
Kalman Filter Gain Calculation	$K_k = P_k^- H_k^T \left(H_k P_k^- H_k^T + R_k\right)^{-1}$
Measurement Update Equations	$x_k^+ = x_k^- + K_k (Z_k - H_k x_k^-)$
	$P_k^+ = P_k^- - K_k H_k P_k^-$

, where

x : State vector

P : State covariance matrix

Φ : State transition matrix

Q : Process noise covariance matrix

R : Measurement noise covariance matrix

Z : Measurement

H : Measurement matrix

Because the algorithm is implemented using error states, the current quaternion and inertial angular velocity should be corrected after the error estimation. The correction operation is performed by the following equations:

$$q_{corrected} = \delta q \otimes q_{estimated} \tag{14}$$

$$\omega_{corrected} = \delta \omega + \omega_{estimated} \tag{15}$$

GPS Only Case:

Instead of using only GPS observations, known dynamics is integrated to the system in order to get a better solution. For this purpose, an Extended Kalman Filter is designed using error quaternion and angular velocity states.

$$\delta x = [\delta q_1\ \delta q_2\ \delta q_3\ \delta w_1\ \delta w_1\ \delta w_1]^T \tag{16}$$

Although a quaternion is composed of four parameters, only the three of them is independent. Therefore, in this study, only the three of them (vector part) is included to the state vector in order to decrease the computational load. After the three components are estimated, the forth one is calculated as:

$$\delta q_4 = \sqrt{1 - \delta q_1{}^2 - \delta q_2{}^2 - \delta q_3{}^2} \tag{17}$$

The system model should be linearized using the first order Taylor series expansion

$$F(x,t) = \left.\frac{\partial f(x,t)}{\partial x}\right|_{\hat{x}(t)} \tag{18}$$

Then, the discrete time state transition matrix, Φ, is calculated as:

$$\Phi_k \approx 1 + \Delta t F \tag{19}$$

In order to update the state vector estimate with the measurements, it is necessary to know how the measurements change with the states. In other words, the function of measurement model should be driven. The measurement matrix, H, represents this relation of the range difference measurements to the quaternion and angular velocity states such that:

$$H = \begin{bmatrix} \frac{\partial Z}{\partial \delta q} & \frac{\partial Z}{\partial \delta \omega} \end{bmatrix} \tag{20}$$

In the equations above Z represents the measurement innovation (δr) and it is equal to:

$$Z = \delta r = \Delta r - \Delta \hat{r} \tag{21}$$

$$\Delta r = (b^B)^T R_I^B e^I \tag{22}$$

$$\Delta \hat{r} = (b^B)^T \hat{R}_I^B e^I \tag{23}$$

,where Δr represents the delta range measured by the GPS receiver, $\Delta \hat{r}$ represent the estimated delta range and $R_I^B = \delta R_I^B \hat{R}_I^B$

By definition, the quaternion error δq is just one half of the small Euler rotations. Then the rotation matrix difference, δR_I^B, can be approximated as:

$$\delta R_I^B \approx I_{3\times3} - 2[\delta q \wedge] \tag{24}$$

After inserting these equations into eq.(21), the final form of the measurement innovation becomes:

$$\delta r = -2(b^B)^T [\delta q \wedge] \hat{R}_I^B e^I = \left\{ -2\left(\hat{R}_I^B e^I\right)^T [b^B \wedge] \right\} \delta q \tag{25}$$

Finally, the measurement matrix is found as:

$$H = \left[-2\left(\hat{R}_I^B e^I\right)^T [b^B \wedge] \quad 0_{3\times3} \right] \tag{26}$$

This matrix should be calculated for every baseline and for each satellite during the flight.

GPS/Gyro Integrated Case

An integrated GPS receiver and three-axis gyro assembly is also considered in this study in order to overcome the problems of standalone GPS case which is mentioned before. The algorithm flow chart is given in Figure 5. The algorithm again is composed of time update and measurement update phases. Note that the Kalman gain is calculated in the measurement update phase. As it can be seen from the algorithm flow chart, the states are updated for both GPS and gyroscope measurements. However, the GPS measurement update is carried out at 1Hz, while the gyro measurement update is at 100Hz. Moreover, the algorithm checks whether the GPS measurements is available or not. If there is no GPS measurement at that time interval, the states are updated only with the gyro measurements.

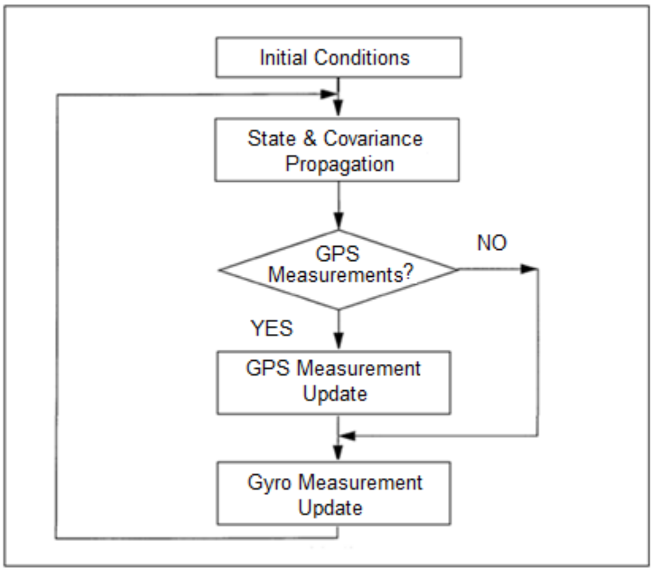

Figure 5: GPS/Gyro Integration Filter Algorithm Flow Chart

One of the differences with the GPS only EKF solution is the addition of three more states into the state vector. In the GPS/Gyro integrated solution, the error state vector is composed of three quaternion components, three inertial angular velocities in body axis and three gyro bias drift states.

$$\Delta x = [\delta q_1\ \delta q_2\ \delta q_3\ \delta\omega_1\ \delta\omega_2\ \delta\omega_3\ b_1\ b_2\ b_3]^T \tag{27}$$

The bias drift error of a gyroscope can be represented by a 1st order Gauss-Markov process.

$$\dot{b}_{Gyro} = -\frac{1}{\tau_{Gyro}} b_{Gyro} + w_{Gyro} \tag{28}$$

,where $\mathrm{w_{Gyro}}$ is the zero mean Gaussian white noise. This term is also called as the driven noise.

Then the new continuous time system model can be written as:

$$\begin{bmatrix} \dot{x}_{old} \\ \dot{b}_1 \\ \dot{b}_2 \\ \dot{b}_3 \end{bmatrix} = \begin{bmatrix} F_{old} & 0 & 0 & 0 \\ 0 & -1/\tau_{Gyro,1} & 0 & 0 \\ 0 & 0 & -1/\tau_{Gyro,2} & 0 \\ 0 & 0 & 0 & -1/\tau_{Gyro,3} \end{bmatrix} \begin{bmatrix} x_{old} \\ b_1 \\ b_2 \\ b_3 \end{bmatrix} \tag{29}$$

,where $\mathrm{x_{old}}$ and $\mathrm{F_{old}}$ represents the states and state transition matrix in eq.(16) and eq.(19) respectively.

The other difference is in the measurement model. In this filter, not only GPS differential phase measurements but also the gyro measurements in three axes are used in the measurement model.

The measurement matrix, H_{GPS}, represents the relation between the range difference measurements and the Kalman Filter states, namely, quaternions, inertial angular velocity and the gyro measurement bias drift.

$$H_{GPS} = [H_{q,GPS} \quad H_{\omega,GPS} \quad H_{b,GPS}] \tag{30}$$

The relation with quaternions and the inertial angular velocities is given in eq.(26). Because there is no relation between the gyro measurement bias drift and the GPS measurements, the new term $H_{b,GPS}$ is equal to zero for all three axes.

The measurement matrix, H_{Gyro}, represents the relation between the range difference measurements and the Kalman Filter states:

$$H_{Gyro} = [H_{q,Gyro} \quad H_{\omega,Gyro} \quad H_{b,Gyro}] \tag{31}$$

In order to determine the elements of the gyro measurement matrix, the measurement innovation should be determined firstly. The measurement innovation, $\delta\omega_{Gyro}$, is the difference between the measured angular velocity and the estimated angular velocity.

$$\delta\omega_{Gyro} = \left(\omega_{IB}^{B} + b_{gyro}\right) - \hat{\omega}_{IB}^{B} \tag{32}$$

,where $\left(\omega_{IB}^{B} + b_{gyro}\right)$ represents the measured angular velocity, while $\hat{\omega}_{IB}^{B}$ represents the estimated one.
After rearranging the equation, the measurement innovation is found as:

$$\delta\omega_{Gyro} = \delta\omega_{IB}^{B} + b_{Gyro} \tag{33}$$

Then by using this equation, the elements of the measurement matrix are found as:

$$H_{Gyro} = [0_{3\times3} \quad I_{3\times3} \quad I_{3\times3}] \tag{34}$$

SIMULATION RESULTS

In this section, the simulation results are shown. Two cases are presented. The first case involves a solution where at least five GPS satellites are always in view. In the second case, a scenario with two GPS outages in the periods between 1500 – 1800 and 4000 – 4300 seconds is applied. Both the GPS only and GPS/Gyro integrated algorithms are tested for these cases. These test cases analyze the performance of the GPS based attitude determination system under the measurement errors, namely receiver noise and multipath error. The results are summarized in Table 3.

Table 3: Performance Parameters Obtained for the Different Test Cases

	Without GPS Outages			**With GPS Outage**		
	Roll	Pitch	Yaw	Roll	Pitch	Yaw
GPS Only Case						
RMS [degrees]	0.1111	0.0790	0.0983	0.1103	0.1246	0.0997
Maximum Error [degrees]	0.3560	0. 2110	0.3616	0.3590	0.6112	0.3616
GPS/Gyro Integrated Case						
RMS [degrees]	0.1094	0.0750	0.0953	0.1100	0.0749	0.0994
Maximum Error [degrees]	0.3339	0.1922	0.3313	0.3339	0.1922	0.3313

Figure 6 represents the magnitude of error in the estimated Euler angles for the first test case. It is observed that the maximum attitude error for the case without GPS outages is below 0.4 degree, while the RMS value is below 0.12 degree for all the angles (Table 3).

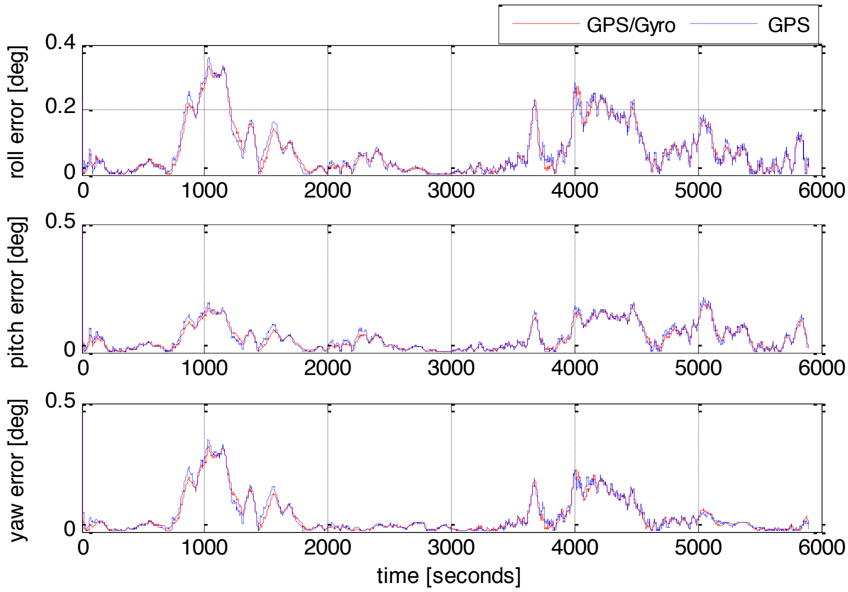

Figure 6: Error Magnitude in the Estimated Euler Angle for the case without GPS Outages

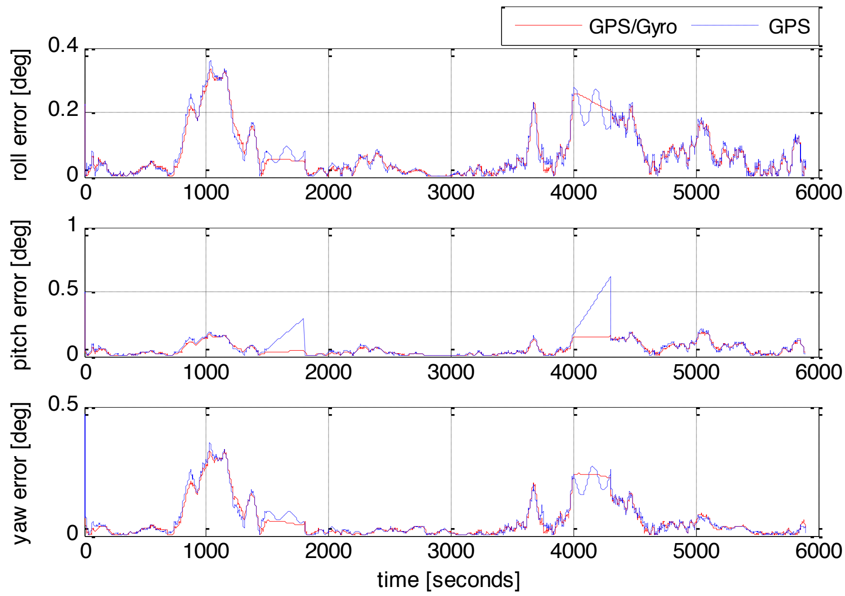

Figure 7: Error Magnitude in the Estimated Euler Angle for the case with GPS Outages

By comparing the results for the GPS only and GPS/Gyro integrated solutions, it is also observed that only a small improvement is obtained with the gyro aiding. However, Figure 7 illustrates that the effect of gyro aiding is seen especially for the cases with GPS outages. The maximum error in the Euler angles for the second case obtained by the GPS only solution is 0.3590, 0.6112 and 0.3616 degrees respectively (Table 3). Aiding the system with the gyroscopes improves the pitch angle accuracy significantly. The improvement is especially seen in the maximum pitch angle error. This error is decreased more than 0.4 degrees with gyro aiding. The effect of gyro aiding on the other angles, roll and yaw, is seen again mostly on the error peaks. However, due to the slow and sinusoidal attitude dynamics of these angles, there is only a small improvement in these angles.

The error increase during the GPS outages is highly affected by the satellite attitude dynamics. This effect can be seen from the high pitch error peaks when the GPS measurements are not available. The maximum error in the pitch angle is about 0.6 degrees, while it is around 0.36 degrees for the other angles. This high difference is due to the high angular velocity in the y-axis. In a one period of the satellite flight, the pitch angle varies between +/-50 degrees, while this value is +/-10 degrees for the roll and yaw angles, as it can be seen in Figure 2. The other effect on the maximum attitude error during the GPS outages is the initial condition error (the error at the beginning of the outage period). The pitch angle error is lower for the first outage period; therefore, the pitch error after the same amount of time is lower for that outage period.

The covariance characteristics of the Kalman Filter states are also examined in this study. Figure 8 shows the estimation error and the corresponding standard deviation of the quaternion states under GPS outages. The standard deviation values are calculated as the square root of the state covariance. It is observed that the gyro aiding decreases the uncertainty on the state estimation especially during the outage periods. It is also observed that the uncertainty in the states during the outage periods is increasing as it is expected to.

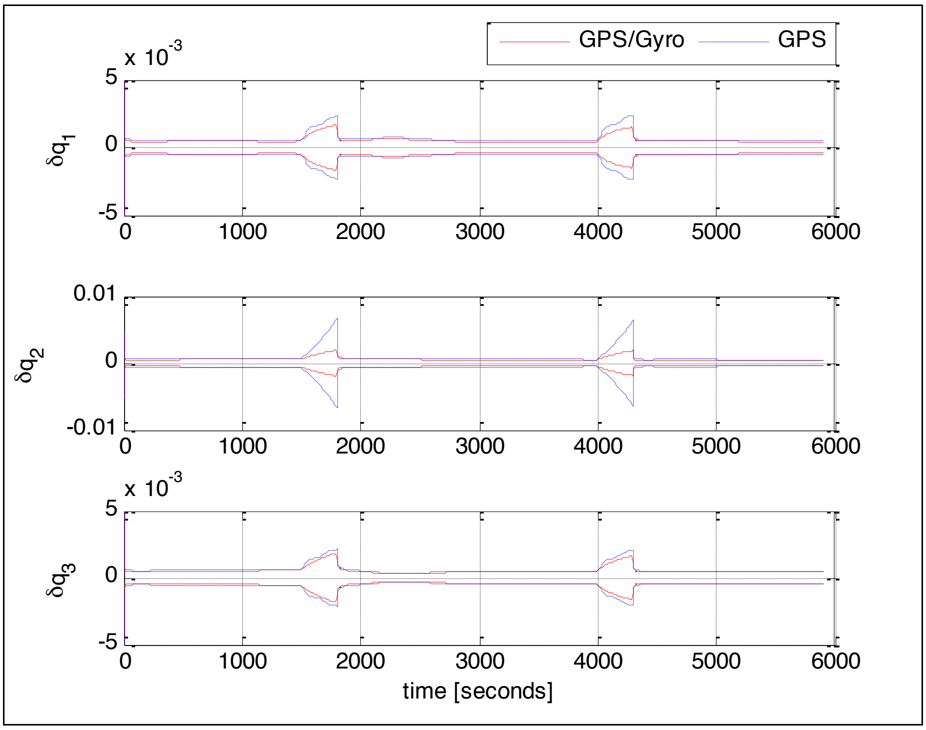

Figure 8: Standard Deviations of the Quaternion States under GPS Outages

CONCLUSION

The goal of this study has been to develope a GPS based attitude determination system for a spacecraft. As the estimation algorithm for attitude determination, an EKF was developed. The algorithms was also modified for the gyro aiding case. The performance improvement obtained with the gyro aiding was analyzed under different GPS visibility cases by including some stochactic GPS errors, namely multipath and receiver noise.

After the simulations tests, the maximum attitude error obtained by using the GPS differential range measurements was found as less than 0.4 degrees. During this test, it was assumed that measurements from five satellites are constantly available througout the flight. The improvement caused by the gyro aiding was observed for the case with GPS outages. The improvement was observed for all the angles but especially in the pitch angle. This is because the angular velocity is quite high in the y-axis compared to the other axes.Therefore, it can be concluded that the gyro integration is essential for the cases with high angular velocities, such as spinning satellites. However, the improvement is small for the stabilized satellites.

References

Anton, H.,Damaren, C., Forbes, J.R. *Spacecraft Dynamics and Control: An Introduction*, UK: John Wiley and Sons, 2013

Bak, T., *Spacecraft Attitude Determination - a Magnetometer Approach*, Ph.D. dissertation, Department of Control Engineering, Aalborg University, Aalborg, Denmark, 1999.

Brady, T.M, *Expanding the Spacecraft Application Base with MEMS Gyros*, The Draper Technology Digest, Vol.16, 2012.

Groves, P., *Principles of GNSS, Inertial, and Multisensor Integrated Navigation Systems*, US: Artech House, 2008.

Khanafseh, S., Langel, S., Pervan, B., *Overbounding Position Errors in the Presence of Carrier Phase Multipath Error Model Uncertainty*, Proceedings of IEEE/ION PLANS 2010, 2010, pp. 575-584.

Lightsey, E.G., *Relative Attitude Determination of Earth Orbiting Formations Using Global Positioning System Receivers*, 2nd International Symposium on Formation Flying Missions & Technologies, Sep 2004

Titterton, D. H., Weston, J. L., Strapdown Inertial Navigation Technology, Stevenage, UK: IEE, 2004.